

Mechanism for reactive chemistry at metal-semiconductor interfaces

R. A. Butera and C. A. Hollingsworth

Department of Chemistry, University of Pittsburgh, Pittsburgh, Pennsylvania 15260

(Received 18 September 1987)

A model based on the balance between the thermodynamic driving force and the kinetic limitation due to atomic and thermal diffusion is presented which can extract quantitative information on the mechanism governing reactive solid interfaces such as occur in many metal-semiconductor systems. The model is used to develop equations which fit the photoelectron intensity data available for the V/Ge(111) system as a function of temperature. We show that the composition and densities of the reaction products can be obtained and that the compound formed is the same as one reported in the bulk phase diagram. Predictions are made as to the effect of the substrate thermal conductivity on the extent of the interfacial region.

INTRODUCTION

The chemical and physical properties of metal-semiconductor interfaces have been the subject of considerable experimental and theoretical interest.¹⁻¹³ Although numerous studies have sought an understanding of the chemistry of these reactive interfaces, and great progress has been made, we are still far from being able to quantitatively understand the mechanism controlling their formation. The understanding of these interesting and important systems is being advanced by the ongoing investigations of the reactivity of the constituents; the thermal and environmental stabilities of interfaces; their electrical behaviors; and the composition, spatial extent, and morphology of an interface at each stage of its development. The work presented in this paper is focused on the mechanism underlying the chemistry occurring within the interfacial region.

When an incoming reactant atom, or molecule, arrives at the surface of a solid second reaction partner and reaction occurs, heat is released, causing a thermal fluctuation. The maximum temperature within the fluctuation region will be some value we will call T^* . While the temperature is greater than the minimum necessary to activate atomic diffusion, T' , diffusion of atoms from both reactants can occur across the products formed at the interface. The temperature of the fluctuation will decay from T^* to T' due to the heat loss into the solid substrate. The rate of heat transfer will be governed by both the thermal diffusivity of the substrate and the thermal gradient. Thus, the time available for atomic diffusion and reaction will be governed by a balance between the thermodynamic driving force and the kinetic limitation due to the atomic and thermal diffusion. We present below a model based on this balance to account for the chemical evolution of products within the solid interface separating the reactants. The model is then used to develop equations to fit the intensity-attenuation curves obtained from photoelectron spectroscopic investigations of the V/Ge(111) interface produced as a function of substrate temperatures.¹⁴

THE MODEL

It is assumed that the chemical reaction takes place at the two boundaries, $\bar{\Theta}$ and $\hat{\Theta}$, of the metal-semiconductor interface and multiple phases can coexist (see Fig. 1). At the semiconductor boundary, $\bar{\Theta}$, the first phase is always produced. At the metal boundary, $\hat{\Theta}$, the products depend on the amount of metal deposited in $\bar{\Delta}, \bar{\Theta}$. We assume that the composition at positions between these boundaries remain fixed at the values produced when the metal was deposited at those positions.

In order for the reactions to take place at the two boundaries there must be diffusion of semiconductor from its boundary and, simultaneously, diffusion of metal in the opposite direction. We assume that the distance through which these diffusions must take place (the distance between the two boundaries) is proportional to $\bar{\Theta}$.

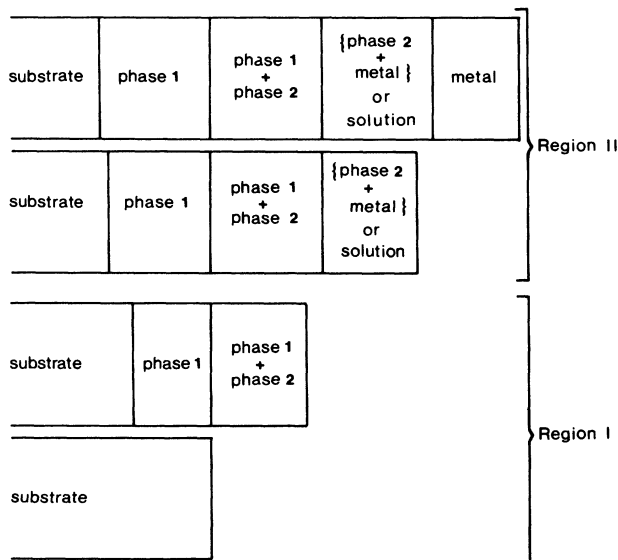


FIG. 1. Schematic representation of the interfacial regions corresponding to the discussion in the text.

The diffusion is reaction activated, and we assume that it is activated by the reaction at the metal boundary. The activation produced by a metal atom is assumed to have a lifetime τ , and the required diffusion must take place in the time τ . At the metal boundary, production of phase 1 requires more diffusion than production of phase 2. The probability that the necessary diffusion takes place in time τ to produce phase i at $\hat{\Theta}$ (the position of the metal boundary when the amount of metal deposited is Θ) can be expressed as (see Appendix A)

$$P_i(\Theta) = f_i(\Theta) \exp(-a_i \Theta^2), \quad (1)$$

where

$$a_i = \beta^2 / (4D_i \tau), \quad (2)$$

and D_i and τ are the diffusion constant and activation lifetime. β is the proportionality constant relating Θ to the diffusion distance (see Appendix C). The function $f_i(\Theta)$ is a weak function of Θ and, for our purpose, can be taken to be a constant (see Appendix A).

We complete our model by making the following assumptions. Phase 1 is more stable, and as much of it is produced as is allowed by diffusion. The remainder of the product is phase 2. When the diffusion distance becomes too great, either not all of the deposited metal can react and some unreacted metal remains, or a metal-rich solution is formed with the composition of semiconductor decreasing with increasing Θ . We identify the relative amount of phase i produced at $\hat{\Theta}$ with $P_i(\Theta)$ as given by Eq. (1).

In line with these assumptions we divide the range of Θ

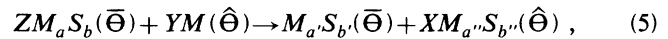
into two regions (see Fig. 1): region I, in which all of the metal reacts to form products with definite compositions, and region II, in which either some of the metal remains unreacted or a variable composition solution is formed. This leads to the following equations, where $P_i(\Theta)$ with $i = 1, 2, m$ represents the relative amount of phase i produced at $\hat{\Theta}$, and $i = m$ refers to the unreacted metal:

$$\begin{aligned} P_1(\Theta) &= \exp(-a_1 \Theta^2), \quad \text{regions I and II} \\ P_2(\Theta) &= 1 - P_1, \quad \text{region I} \\ P_2(\Theta) &= A_2 \exp(-a_2 \Theta^2), \quad \text{region II} \\ P_m(\Theta) &= 1 - P_1 - P_2, \quad \text{region II.} \end{aligned} \quad (3)$$

The parameter A_2 allows matching of the two forms of P_2 at the transition between regions I and II, where

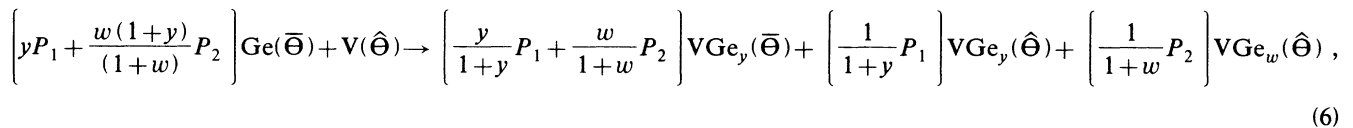
$$1 - \exp(-a_1 \Theta^2) = A_2 \exp(-a_2 \Theta^2). \quad (4)$$

We shall treat a general case and then specialize it for our particular application. We write the reaction as



which means Z moles of $M_a S_b$ at position $\bar{\Theta}$ (the semiconductor boundary) in the interface reacts with Y moles of M from $\hat{\Theta}$ (where the metal is being deposited) to give one mole of $M_a' S_b'$ at $\bar{\Theta}$ and X moles of $M_{a''} S_{b''}$ at $\hat{\Theta}$.

Atom balance and an assumption about spatial continuity of the solid at $\bar{\Theta}$ allows us to obtain expressions for the stoichiometric coefficients (X, Y, Z) in terms of $a, b, a', b', a'',$ and b'' (see Appendix B). The result for the specific case of the V/Ge interface can be expressed as



where $P_1, P_2,$ and P_m are given by Eq. (3).

In order to derive the equations necessary to describe the photoelectron-intensity-attenuation results, we consider the notation given in Fig. 2.

Let \bar{N}_T be the total atoms in the single-phase portion (produced at $\bar{\Theta}$), \hat{N}_T the total atoms in the two-phase portion (produced at $\hat{\Theta}$), $N_T (= \bar{N}_T + \hat{N}_T)$ the total atoms in the interface, and $N_m (= \Theta/\gamma)$ the atoms of metal deposited, where

$$\Theta = |\bar{\Theta}| + |\hat{\Theta}|,$$

the average length of a metal atom in \AA is

$$\gamma = \left[\frac{M_m \times 10^{24}}{\rho_m N_0} \right]^{1/3},$$

and M_m is the atomic weight of the metal, ρ_m is the bulk

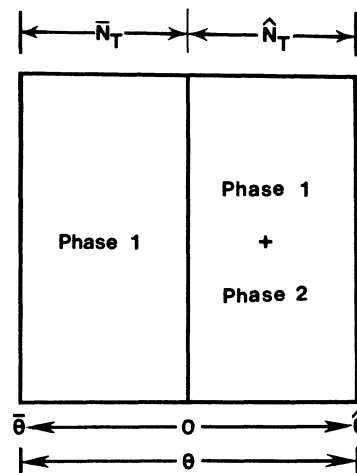


FIG. 2. Schematic representation of the interfacial portions within region I. $\bar{\Theta}$ and $\hat{\Theta}$ are, respectively, the semiconductor and metal boundaries of the interface when the amount of metal that has been deposited is Θ .

density of the metal, and $N_0 = 6.02 \times 10^{23}$. For vanadium, $\gamma = 2.4$. Therefore,

$$N_m(\Theta) = \Theta / 2.4, \quad (7)$$

where Θ is measured in Å. The expressions for the photoelectron intensities when the amount of metal that has been deposited is Θ^f are (see Appendix C)

$$\frac{I_{\text{Ge}_{(1)}}(\Theta^f)}{I_{\text{Ge}_{(S)}}(0)} = \frac{y}{1+y} \frac{\rho_1}{Aw_V + yAw_{\text{Ge}}} \left[\left\{ 1 - \exp[-\bar{N}_T(\Theta^f)/\lambda] \right\} \exp[-\Theta^f/(\gamma\lambda)] + \frac{1}{\gamma\lambda} \int_0^{\Theta^f} \exp(-a_1\Theta^2) \exp\left[-\frac{\Theta^f-\Theta}{\gamma\lambda}\right] d\Theta \right], \quad (8)$$

$$\frac{I_{\text{Ge}_{(2)}}(\Theta^f)}{I_{\text{Ge}_{(S)}}(0)} = \frac{w}{1+w} \frac{\rho_2}{Aw_V + wAw_{\text{Ge}}} \left\{ \frac{1}{\gamma\lambda} \left[\int_0^{\Theta^f} \exp\left[-\frac{\Theta^f-\Theta}{\gamma\lambda}\right] d\Theta - \int_0^{\Theta^f} \exp(-a_1\Theta^2) \exp\left[-\frac{\Theta^f-\Theta}{\gamma\lambda}\right] d\Theta \right] \right\}, \quad (9)$$

and

$$\frac{I_{\text{Ge}_{(S)}}(\Theta^f)}{I_{\text{Ge}_{(S)}}(0)} = \alpha \left\{ \left\{ 1 - \exp[-\bar{N}_T(\Theta^f)/\lambda] \right\} \exp[-\Theta^f/(\gamma\lambda)] + \frac{1}{\gamma\lambda} \int_0^{\Theta^f} \exp(-a_1\Theta^2) \exp\left[-\frac{\Theta^f-\Theta}{\gamma\lambda}\right] d\Theta \right\} + \exp[-\bar{N}_T(\Theta^f)/\lambda] \exp[-\Theta^f/(\gamma\lambda)], \quad (10)$$

where λ is the attenuation length in atoms, $\gamma\lambda = \lambda_0$ is the Seah-Dench attenuation length in Å,¹⁵ and $I_{\text{Ge}_{(S)}}(0)$ is the intensity from the substrate Ge at $\Theta = 0$. We associate the term multiplied by α in Eq. (10) with the Ge emission from a solution of V in Ge, which is most likely located at the grain boundaries within the reacted region as suggested by Butera, del Giudice, and Weaver (BGW),¹⁴ and the last term accounts for the emission from the substrate.

DISCUSSION

Butera, del Giudice, and Weaver¹⁴ have fitted high-resolution photoemission results for the V/Ge(111) interface over the temperature region 300–643 K for coverages up to 60 Å of vanadium using a model based on the production of separate phases, the amount of each governed by a linear lever rule. Their model represents a first step in the quantitative description of these interfaces. However, the BGW model does not yield density information for the phases and also introduced material specific electron attenuation lengths for each phase.

The model we presented above does not require the introduction of material-specific electron attenuation lengths and does provide density information, as well as insight into the mechanism controlling the chemistry of these interfaces. We have applied our model to the above-mentioned data and the results are shown in Figs.

3–8. As can be seen from Fig. 3, the data can be fitted quite well using the composition and density of the bulk compound,¹⁶ $\text{VGe}_{1.8}$ and $\rho = 7.07 \text{ g/cm}^3$, for the first reaction product and the composition $\text{VGe}_{0.06}$ and a density approximately the same as pure vanadium for the second reaction product. It is our belief that the $\text{VGe}_{0.06}$ material represents the saturated Ge-in-V solution. The data for elevated temperatures have been fitted using our model with only the parameters α and a_1 changing with temperature (Figs. 4–8). The parameters used are given in Table I.

Butera, del Giudice, and Weaver¹⁴ have shown that the relative amount of the V-in-Ge solution present at the grain boundaries appears to be independent of Θ but dependent on T in the following manner:

$$\alpha = B \exp(-E_\alpha/RT). \quad (11)$$

Since $a_1 = 1/(4D\tau)$ and $D = D_0 \exp(-E^*/RT)$, we predict that the temperature dependence of a_1 will be given by

$$\ln a_1 = (E^*/RT) + \text{const}. \quad (12)$$

Figure 9 shows that Eq. (12) does represent the temperature dependence of a_1 and we obtain an activation energy, E^* , of 7.79 kcal/mol for the diffusion occurring during the activation. We now consider how this value of the activation energy compares with that reported by

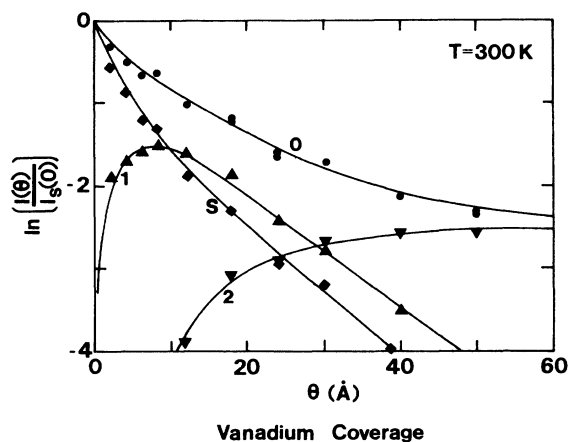


FIG. 3. Ge 3d core-level attenuation curve, $T_{\text{substrate}} = 300$ K. The notation used in this figure and Figs. 4–8 is as follows: 1, phase-1 Ge emission; 2, phase-2 Ge emission; α denotes V-in-Ge-solution Ge emission; S denotes substrate Ge emission; 0 denotes total Ge emission.

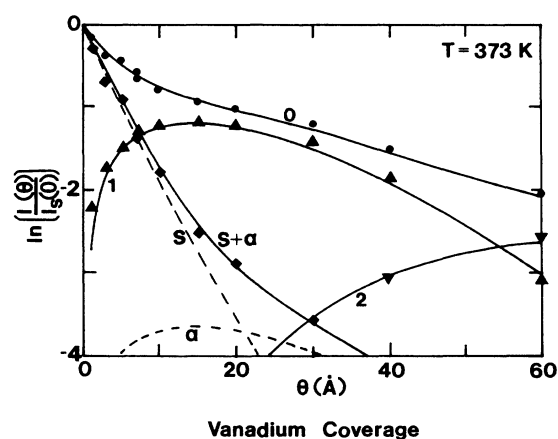


FIG. 4. Ge 3d core-level attenuation curve, $T_{\text{substrate}} = 373$ K.

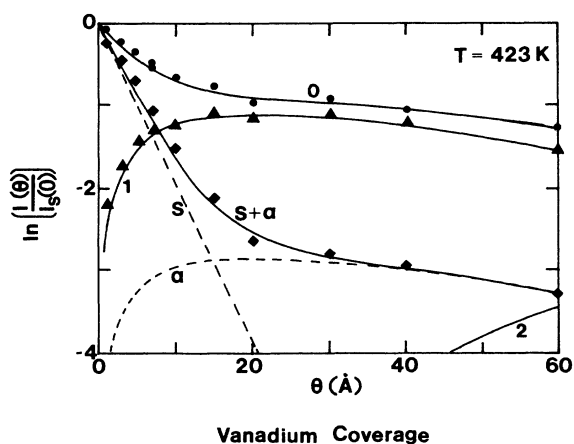


FIG. 5. Ge 3d core-level attenuation curve, $T_{\text{substrate}} = 423$ K.

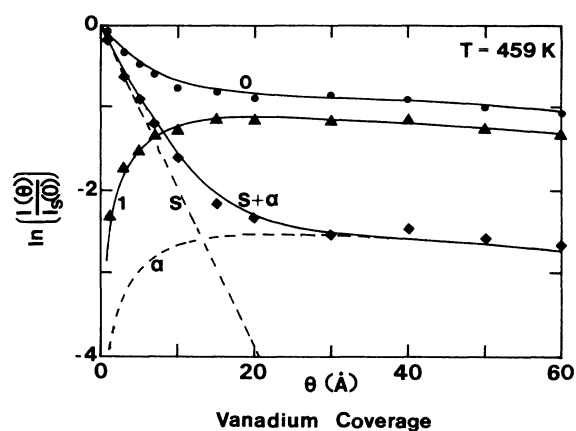


FIG. 6. Ge 3d core-level attenuation curve, $T_{\text{substrate}} = 459$ K.

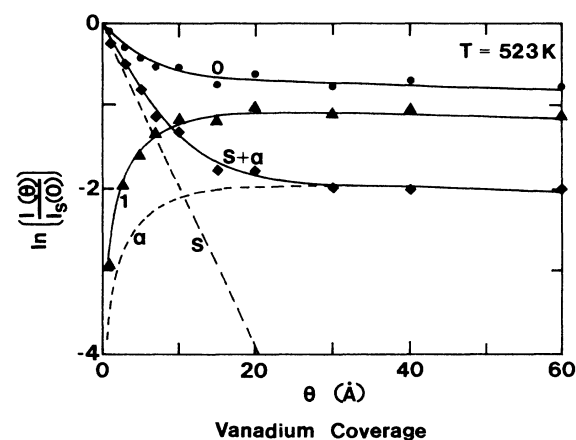


FIG. 7. Ge 3d core-level attenuation curve, $T_{\text{substrate}} = 523$ K.

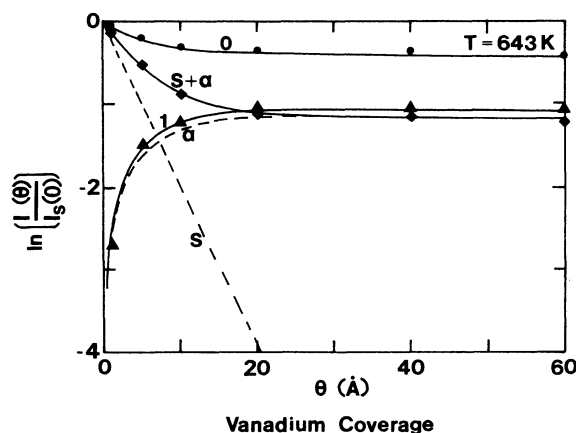


FIG. 8. Ge 3d core-level attenuation curve, $T_{\text{substrate}} = 643$ K.

TABLE I. Parameters used to obtain fits between Eqs. (44)–(46) and the experimental results of BGW (Ref. 14). Temperature-independent parameters used in the fitting included the atomic photoelectron mean free path $\lambda=6$ (where $\gamma\lambda=\lambda_0$, the Seah-Dench mean free path); the composition and density for $VGe_{1.8}$ ($y=1.8$ and $\rho_1=7.07$ g/cm³); the composition and density for the Ge-in-V solution ($w=0.06$ and $\rho_2=6.1$ g/cm³); and the densities and atomic weights of V and Ge ($\rho_V=6.1$ g/cm³, $\rho_{Ge}=5.36$ g/cm³, $A_{wV}=50.94$, $A_{wGe}=72.60$). Temperature-dependent parameters are $a_1=1/(4D\tau)$ and the amount of the V-in-Ge solution, α .

T (K)	$a_1=1/(4D\tau)$ (Å ⁻²)	α
300	1.39×10^{-2}	
373	1.25×10^{-3}	0.030
423	2.22×10^{-4}	0.060
459	1.07×10^{-4}	0.082
523	3.68×10^{-5}	0.141
643	9.3×10^{-6}	0.319

BGW (Ref. 14) using their linear-lever-rule model. The relationship between P_1 , used in our model, and $1-\chi$, used in the BGW linear-lever-rule model, is shown in Fig. 10. In the BGW model,

$$1-\chi = \frac{\Theta_1^* - \Theta}{\Theta_1^* - \Theta_2}, \quad (13)$$

where Θ_i is the coverage at which phase i begins to form and Θ_i^* is the coverage at which phase i ceases to form. We can now write

$$P_1 \approx \frac{\Theta_1^* - \Theta}{\Theta_1^* - \Theta_2} \quad (14)$$

for the region of Θ near the point of inflection in P_1 . Thus,

$$\exp(-a_1\Theta^2) \approx \frac{\Theta_1^* - \Theta}{\Theta_1^* - \Theta_2} \quad (15)$$

and

$$\begin{aligned} \frac{d \exp(-a_1\Theta^2)}{d\Theta} &= -2a_1\Theta \exp(-a_1\Theta^2) \\ &\approx \frac{d}{d\Theta} \frac{\Theta_1^* - \Theta}{\Theta_1^* - \Theta_2} \\ &= -\frac{1}{\Theta_1^* - \Theta_2}, \end{aligned} \quad (16)$$

yielding

$$2a_1\Theta \exp(-a_1\Theta^2) \approx \frac{1}{\Theta_1^* - \Theta_2}. \quad (17)$$

Let $\Theta = \Theta_{inf}$ at the point of inflection of $\exp(-a_1\Theta^2)$; then,

$$\frac{d^2 \exp(-a_1\Theta^2)}{d\Theta^2} = (2a_1\Theta^2 - 1)2a_1 \exp(-a_1\Theta^2) = 0 \quad (18)$$

and

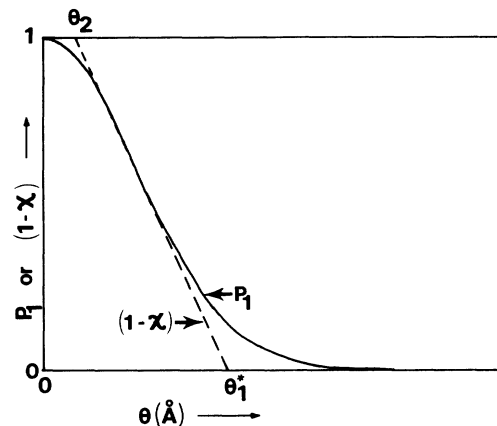


FIG. 9. Arrhenius plot of $\ln a_1$ vs $1/T$ for the V/Ge(111) interface.

$$\Theta_{inf} = (2a_1)^{-1/2}. \quad (19)$$

We now fit the magnitude and slope at Θ_{inf} to yield

$$(\Theta_1^*)^2 = 2/a_1. \quad (20)$$

Thus,

$$(\Theta_1^*)^2 = 8D_0\tau \exp\left[-\frac{E^*}{RT}\right] \quad (21)$$

and

$$\ln \Theta_1^* = \ln(8D_0\tau)^{1/2} - \frac{E^*}{2RT}. \quad (22)$$

Since BGW (Ref. 14) fitted $\ln \Theta_1^*$ versus $1/T$ to obtain their reported activation energy, their value is thus equal to $E^*/2$. The value of the activation energy reported by BGW (Ref. 14) is 3.93 kcal/mol, which corresponds to a value of $E^*=7.86$ kcal/mol. This is the same as the value we obtain within experimental error.

We can get some idea of the nature of τ and possibly, a rough estimate of the values of τ and D by following considerations. Let T^* be the highest temperature that

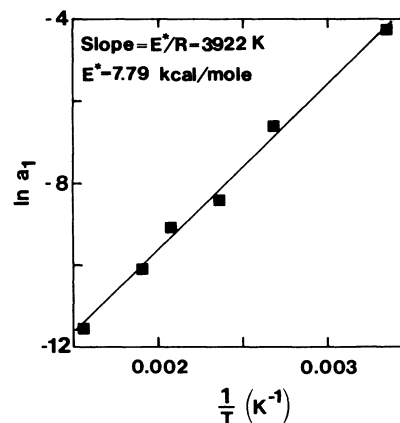


FIG. 10. Relationship between P_1 used in this model and the linear level used by BGW.

occurs during the activation, and T' be the temperature below which significant diffusion cannot take place. T' is independent of T , but T^* is a function of T , viz.,

$$T^* = T + \Delta T_a, \quad (23)$$

where ΔT_a is the maximum fluctuation in temperature produced by the reaction. A single-relaxation-time approximation for the temperature decay due to heat leak from the interface into the bulk substrate gives

$$\Delta T = \Delta T_a \exp(-at), \quad (24)$$

where $\Delta T = T - T_s$, $\Delta T_a = T^* - T_s$, and T_s is the temperature of the bulk substrate.

Since τ is the time required for the temperature of the fluctuation to decrease from T^* to T' , we have

$$T' - T_s = (T^* - T_s) \exp(-a\tau) \quad (25)$$

and

$$\tau = (1/a) \ln[(T^* - T_s)/(T' - T_s)]. \quad (26)$$

The constant a is of the form

$$a = \eta \kappa l^{-2}, \quad (27)$$

where κ is the thermal diffusivity, and l is the linear dimension of the fluctuation. The constant η depends on the shape of the fluctuation, but does not vary greatly. A reasonable set of values for the V/Ge(111) system might be

$$\eta \approx 10,$$

$$l^2 \approx 10^{-11} \text{ cm}^2,$$

$$\kappa \approx 10^{-3} \text{ cm}^2/\text{s},$$

and

$$(T^* - T_s)/(T' - T_s) \approx 2.$$

These values give $\tau \approx 10^{-9}$ s and $D \approx 10^{-6}$ cm²/s.

τ increases with T_s and, in fact, should become infinite when T is sufficiently high that the activated diffusion occurs spontaneously. Equation (26) is in agreement with this, since it gives $\tau \rightarrow \infty$ as $T_s \rightarrow T'$ (see Fig. 11). Thus, our model predicts that for two substrates which differ only in κ and react similarly with the metal to form a product having the same metal-semiconductor composition, the interface extent in Θ will be smaller for the substrate having the larger value of κ . BGW-model fits of the photoelectron intensity attenuation data for the Ce/Si(111) and Ce/Ge(111) interfaces¹² yield the following values:

$$[\text{Ce}]_{\text{Ce-Si}}/[\text{Si}]_{\text{Ce-Si}} = 0.55 \pm 0.05, \quad \Theta_i^* = 9 \text{ \AA} \quad \text{for Ce/Si(111)}$$

and

$$[\text{Ce}]_{\text{Ce-Ge}}/[\text{Ge}]_{\text{Ce-Ge}} = 0.40 \pm 0.05,$$

$$\Theta_i^* = 19 \text{ \AA} \quad \text{for Ce/Ge(111)}.$$

The thermal conductivity of Si is approximately twice that of Ge (Ref. 7) and, assuming that the chemistry of Si and Ge is similar, Eq. (26) would predict that the phase

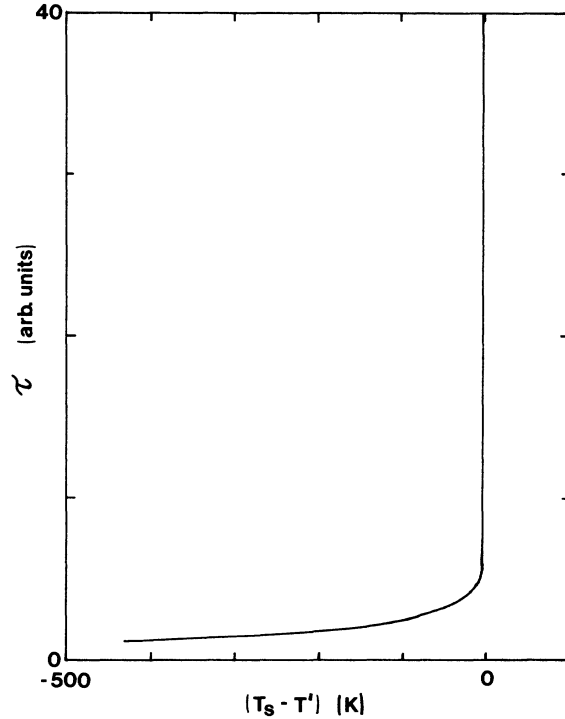


FIG. 11. Temperature dependence of the activation lifetime, τ .

formed with Ge would extend twice as far as that formed with Si. This is consistent with the values of Θ_i^* reported from the BGW-model fits of the experimental data.

In conclusion, we have shown that a model based on the balance between the thermodynamic driving force and the kinetic limitation due to atomic and thermal diffusion can be used to extract quantitative information on the mechanism governing reactive metal-semiconductor interfaces. We are presently extending this approach to the terminal variable composition solution, the metal-binary-semiconductor interface, and also other cases where solid reaction products are formed within the interface between reactants. It is our belief that the mechanism presented here is generally applicable in these cases.

ACKNOWLEDGMENTS

Stimulating discussions with D. Waldeck and E. Faizi are acknowledged.

APPENDIX A: DERIVATION OF EQ. (1)

Since the diffusing atoms are absorbed by reaction once they arrive at the reaction boundaries, we need the probability that an atom arrived at the reaction site for the first time at some time between 0 and τ . The probability that an atom arrives during the time t and $t + dt$ for the first time is proportional to

$$\frac{\Theta}{t^{3/2}} \exp\left[-\frac{\Theta^2}{4Dt}\right] dt. \quad (\text{A1})$$

The probability that we seek is proportional to

$$\int_0^\tau \frac{\Theta}{t^{3/2}} \exp\left[-\frac{\Theta^2}{4Dt}\right] dt \propto \int_u^\infty \exp(-x^2) dx, \quad (\text{A2})$$

where

$$u = \frac{\Theta}{(4D\tau)^{1/2}}. \quad (\text{A3})$$

Use of

$$\frac{2}{\pi^{1/2}} \int_u^\infty \exp(-x^2) dx = 1 - \text{erf}(u) \quad (\text{A4})$$

and

$$\frac{\exp(-u^2)}{u + (u^2 + 2)^{1/2}} < \int_u^\infty \exp(-x^2) dx \leq \frac{\exp(-u^2)}{u + (u^2 + 4/\pi)^{1/2}} \quad (\text{A5})$$

leads to

$$P_i(\Theta) = C [1 - \text{erf}(a_i^{1/2}\Theta)], \quad (\text{A6})$$

which can be put into the form of Eq. (1) with

$$\begin{aligned} \frac{C}{a_i^{1/2}\Theta + (a_i\Theta^2 + 2)^{1/2}} < f_i(\Theta) \\ \leq \frac{C}{a_i^{1/2}\Theta + (a_i\Theta^2 + 4/\pi)^{1/2}}, \end{aligned} \quad (\text{A7})$$

where the equality holds in the limit $\Theta \rightarrow 0$. The function $f_i(\Theta)$ is much weaker than the exponential, and the experimental results can be described by Eq. (1) with $f_i(\Theta)$ equal to a constant.

APPENDIX B: SOME ASPECTS OF THE REACTION-DIFFUSION PROCESS

We obtain the stoichiometric coefficients (X, Y, Z) in terms of $a, b, a', b', a'',$ and b'' as follows. Consideration of atom balance gives

$$Za + Y = a' + Xa'' \quad \text{for metal } M, \quad (\text{B1})$$

$$Zb = b' + Xb'' \quad \text{for semiconductor } S.$$

We next assume that continuity of the solid at $\bar{\Theta}$ after reaction requires that

$$Z(a + b) = q(a' + b'), \quad (\text{B2})$$

where q is constant. Equations (B1) and (B2) lead to

$$\begin{aligned} Z &= q[(a' + b')/(a + b)], \\ X &= (Zb - b')/b'', \end{aligned} \quad (\text{B3})$$

$$Y = a' + [(Zb - b')/b'']a'' - Za.$$

The equations for the diffusion process can be written as

$$\begin{aligned} (Zb - b')S(\bar{\Theta}) &\rightarrow (Zb - b')S(\hat{\Theta}), \\ (a' - Za)M(\hat{\Theta}) &\rightarrow (a' - Za)M(\bar{\Theta}). \end{aligned} \quad (\text{B4})$$

If we assume that $q = 1$ (which gives satisfactory results

for the V/Ge system), then Eq. (B4) becomes

$$\begin{aligned} [(a'b - b'a)/(a + b)]S(\bar{\Theta}) \\ \rightarrow [(a'b - b'a)/(a + b)]S(\hat{\Theta}), \\ [(a'b - b'a)/(a + b)]M(\hat{\Theta}) \\ \rightarrow [(a'b - b'a)/(a + b)]M(\bar{\Theta}). \end{aligned} \quad (\text{B5})$$

For our application ($a = 0$ and $b = 1$) we have

$$\begin{aligned} a'S(\bar{\Theta}) &\rightarrow a'S(\hat{\Theta}), \\ a'M(\hat{\Theta}) &\rightarrow a'M(\bar{\Theta}). \end{aligned} \quad (\text{B6})$$

We shall now consider the specific case of the V/Ge interface. The data for this system corresponds to region I and the reaction-induced diffusion processes involved can be expressed (in terms of per mole of V deposited) as follows:

Production of phase 1 at $\bar{\Theta}$ and $\hat{\Theta}$,

$$y\text{Ge}(\bar{\Theta}) + \text{V}(\hat{\Theta}) \rightarrow \frac{y}{1+y}\text{VGe}_y(\bar{\Theta}) + \frac{1}{1+y}\text{VGe}_y(\hat{\Theta}), \quad (\text{B7})$$

with the diffusion process

$$\begin{aligned} \frac{y}{1+y}\text{Ge}(\bar{\Theta}) &\rightarrow \frac{y}{1+y}\text{Ge}(\hat{\Theta}), \\ \frac{y}{1+y}\text{V}(\hat{\Theta}) &\rightarrow \frac{y}{1+y}\text{V}(\bar{\Theta}). \end{aligned} \quad (\text{B8})$$

Production of phase 1 at $\bar{\Theta}$ and phase 2 at $\hat{\Theta}$,

$$\begin{aligned} \frac{w(1+y)}{1+w}\text{Ge}(\bar{\Theta}) + \text{V}(\hat{\Theta}) \\ \rightarrow \frac{w}{1+w}\text{VGe}_w(\bar{\Theta}) + \frac{1}{1+w}\text{VGe}_w(\hat{\Theta}), \end{aligned} \quad (\text{B9})$$

with the diffusion process

$$\begin{aligned} \frac{w}{1+w}\text{Ge}(\bar{\Theta}) &\rightarrow \frac{w}{1+w}\text{Ge}(\hat{\Theta}), \\ \frac{w}{1+w}\text{V}(\hat{\Theta}) &\rightarrow \frac{w}{1+w}\text{V}(\bar{\Theta}). \end{aligned} \quad (\text{B10})$$

The combination of processes (B7) and (B9) in proper proportion leads to Eq. (6).

APPENDIX C: PHOTOELECTRON INTENSITY EXPRESSIONS

A relationship between $N_T(\Theta)$, the number of atoms in the interface, and $N_m(\Theta)$ can be obtained as follows. From Eq. (23),

$$\frac{dN_T}{dN_m} = (1+y)\frac{w}{1+w} + 1 + \left[y - (1+y)\frac{w}{1+w} \right] P_1, \quad (\text{C1})$$

where P_1 is given by Eq. (3). Using the experimental fit values, $y = 1.8$ and $w = 0.06$ (see the Discussion), we obtain

$$N_T(\Theta) = 1.16(1/2.4)\Theta + 1.64(1/2.4) \int_0^\Theta \exp(-a_1 x^2) dx, \quad (C2)$$

$$N_T(\Theta) = 1.16(1/2.4)\Theta + 1.64(1/2.4)(\frac{1}{2})(\pi/a_1)^{1/2} \times \operatorname{erf}[(a_1\Theta^2)^{1/2}], \quad (C3)$$

and

$$N_T(\Theta)/N_m(\Theta) = 1.16 + 1.64 \left[\frac{\pi}{4a_1\Theta^2} \right]^{1/2} \operatorname{erf}[(a_1\Theta^2)^{1/2}]. \quad (C4)$$

As $(a_1\Theta^2)^{1/2}$ goes from 0 to $2^{1/2}$, which fairly well covers the two-phase region, N_1/N_m gradually decreases from 2.8 to 1.6. Thus, for this region of Θ we can use $N_1/N_m \approx 2.2$, and therefore,

$$N_T(\Theta) = (2.2/2.4)\Theta \approx \Theta. \quad (C5)$$

This means that for this region, in Eq. (2) we can take

$$\beta \approx 1. \quad (C6)$$

For values of Θ corresponding to region II, Eq. (C1) must be modified to account for P_m , but we need not consider that here. Thus, because of Eq. (C5), the diffusion "distance" involved in Eq. (2) is in terms of the number of atoms, N_T , as well as in units of length (\AA).

The reaction equations for the V/Ge interface are

$$P_1 \left[y\operatorname{Ge}(\bar{\Theta}) + V(\hat{\Theta}) \rightarrow \frac{y}{1+y} V\operatorname{Ge}_y(\bar{\Theta}) + \frac{1}{1+y} V\operatorname{Ge}_y(\hat{\Theta}) \right], \quad (C7)$$

$$(1-P_1) \left[\frac{w(1+y)}{(1+w)} \operatorname{Ge}(\bar{\Theta}) + V(\hat{\Theta}) \rightarrow \frac{w}{1+w} V\operatorname{Ge}_y(\bar{\Theta}) + \frac{1}{1+w} V\operatorname{Ge}_w(\hat{\Theta}) \right], \quad (C8)$$

and

$$\frac{d\bar{N}_T}{dN_m} = yP_1 + \frac{w}{1+w}(y+1)(1-P_1) = \left[y - \frac{w}{1+w}(1+y) \right] P_1 + \frac{w}{1+w}(1+y), \quad (C9)$$

$$\bar{N}_T(\Theta^f) = \frac{w}{1+w}(1+y) \frac{\Theta^f}{\gamma} + \left[\frac{y - \frac{w}{1+w}(1+y)}{\gamma} \right] \int_0^{\Theta^f} \exp(-a_1\Theta^2) d\Theta, \quad (C10)$$

where the superscript f indicates the "final" value of a variable of integration, and

$$\frac{d\hat{N}_T}{dN_m} = P_1 + (1-P_1) = 1, \quad (C11)$$

$$\hat{N}_T = N_m = \Theta/\gamma. \quad (C12)$$

Let $\bar{N}_{\operatorname{Ge}(i)}$ be atoms of Ge in phase i in the single-phase portion and $\hat{N}_{\operatorname{Ge}(i)}$ the atoms of Ge in phase i in the two-phase portion. Thus,

$$d\bar{N}_{\operatorname{Ge}(1)} = \frac{y}{1+y} d\bar{N}_T, \quad (C13)$$

$$\begin{aligned} d\hat{N}_{\operatorname{Ge}(1)} &= \frac{y}{1+y} P_1 dN_m \\ &= \frac{y}{1+y} P_1 \frac{d\Theta}{\gamma} \\ &= \frac{1}{\gamma} \frac{y}{1+y} \exp(-a_1\Theta^2) d\Theta, \end{aligned} \quad (C14)$$

$$\begin{aligned} d\hat{N}_{\operatorname{Ge}(2)} &= \frac{w}{1+w} (1-P_1) d\hat{N}_T \\ &= \frac{1}{\gamma} \frac{w}{1+w} [1 - \exp(-a_1\Theta^2)] d\Theta. \end{aligned} \quad (C15)$$

We now obtain the photoelectron intensities by convoluting the number of germanium atoms with the photoelectron attenuation functions to yield

$$\bar{I}_{\operatorname{Ge}(1)}(\Theta^f) = K_1 \left[\int_0^{\Theta^f} \exp[-\bar{N}_T(\Theta)/\lambda] d\bar{N}_{\operatorname{Ge}(1)} \right] \times \exp(-\hat{N}_T/\lambda), \quad (C16)$$

$$\hat{I}_{\operatorname{Ge}(1)}(\Theta^f) = K_1 \int_0^{\Theta^f} \exp\{-[\hat{N}_T(\Theta^f) - \hat{N}_T(\Theta)]/\lambda\} d\hat{N}_{\operatorname{Ge}(1)}. \quad (C17)$$

Also,

$$I_{\operatorname{Ge}(1)}(\Theta^f) = \bar{I}_{\operatorname{Ge}(1)}(\Theta^f) + \hat{I}_{\operatorname{Ge}(1)}(\Theta^f) \quad (C18)$$

and

$$I_{\operatorname{Ge}(2)}(\Theta^f) = K_2 \int_0^{\Theta^f} \exp\{-[\hat{N}_T(\Theta^f) - \hat{N}_T(\Theta)]/\lambda\} d\hat{N}_{\operatorname{Ge}(2)}. \quad (C19)$$

These lead to Eqs. (8)–(10).

- ¹L. J. Brillson, *Surf. Sci. Rep.* **2**, 123 (1982).
- ²J. H. Weaver, in *Analysis and Characterization of Thin Films*, Vol. 28 of *Treatise on Materials Science and Thin Films*, edited by K. N. Tu and R. Rosenberg (Academic, New York, 1987).
- ³G. LeLay, *Surf. Sci.* **132**, 169 (1983).
- ⁴J. R. Waldrop, S. P. Kowalczyk, and R. W. Grant, *J. Vac. Sci. Technol.* **21**, 607 (1982); E. A. Kraut, R. W. Grant, J. R. Waldrop, and S. P. Kowalczyk, *Phys. Rev. B* **28**, 1965 (1983).
- ⁵A. Kahn, *Surf. Sci. Rep.* **3**, 425 (1983).
- ⁶G. A. Prinz, *Phys. Rev. Lett.* **54**, 1051 (1985); S. A. Chambers, F. Xu, H. W. Chen, I. M. Vitomirov, S. B. Anderson, and J. H. Weaver, *Phys. Rev. B* **34**, 6605 (1986).
- ⁷R. R. Daniels, A. D. Katnani, Te-Xiu Zhao, G. Margaritondo, and A. Zunger, *Phys. Rev. Lett.* **49**, 895 (1982); M. Grioni, J. Joyce, S. A. Chambers, D. G. O'Neill, M. del Giudice, and J. H. Weaver, *Phys. Rev. Lett.* **53**, 2331 (1984).
- ⁸R. T. Tung, J. M. Gibson, and J. M. Poate, *Phys. Rev. Lett.* **50**, 429 (1983); M. Liehr, P. E. Schmid, F. K. LeGoues, and P. S. Ho, *ibid.* **54**, 2139 (1985).
- ⁹R. M. Tromp, G. W. Rubloff, and E. J. van Loenen, *J. Vac. Sci. Technol. A* **4**, 865 (1986).
- ¹⁰E. J. van Loenen, J. W. M. Frenken, and J. F. van der Veen, *Appl. Phys. Lett.* **45**, 41 (1984).
- ¹¹W. E. Spicer, I. Lindau, P. Skeath, C. Y. Su, and P. Chye, *Phys. Rev. Lett.* **44**, 420 (1980); P. H. Mahowald, R. S. List, W. E. Spicer, J. Woicik, and P. Pianetta, *J. Vac. Sci. Technol. B* **3**, 1252 (1985).
- ¹²R. A. Butera, M. del Giudice, and J. H. Weaver, *Phys. Rev. B* **33**, 5435 (1986).
- ¹³M. del Giudice, J. J. Joyce, M. W. Ruckman, and J. H. Weaver, *Phys. Rev. B* **32**, 5149 (1985).
- ¹⁴R. A. Butera, M. del Giudice, and J. H. Weaver, *Phys. Rev. B* **36**, 4754 (1987).
- ¹⁵M. P. Seah and W. A. Dench, *Surf. Interface Anal.* **1**, 2 (1979).
- ¹⁶H. Völlenkne, A. Wittmann, and H. Nowotny, *Monat. Chem.* **95**, 1544 (1964); J. F. Smith, *Bull. Alloy Phase Diagrams* **2**, 205 (1981).
- ¹⁷*Thermal Conductivity, Metallic Elements and Alloys*, Vol. 1 of *Thermophysical Properties of Matter*, edited by Y. S. Touloukian, R. W. Powell, C. Y. Ho, and P. G. Klemens (Plenum, New York, 1970).